Stem Cell Rev and Rep (2014) 10:295–303
DOI 10.1007/s12015-013-9492-x

The Size of Mesenchymal Stem Cells is a Significant Cause of Vascular Obstructions and Stroke

Jianfeng Ge · Ling Guo · Shan Wang · Yiling Zhang · Ting Cai · Robert C. H. Zhao · Yaojiong Wu

Published online: 7 January 2014

Abstract
Background and Purpose Intravascular injection of mesenchymal stem cells (MSCs) has been found to cause considerable vascular obstructions which may lead to serious outcomes, particularly after intra-arterial injection. However, the underlying mechanisms have been poorly understood.
Methods In this study, we fractionated MSCs that had been cultured in monolayer for six passages into small (average diameter=17.9 μm) and large (average diameter 30.4 μm) populations according to their sizes, and examined their vascular obstructions after intra-internal carotid artery injection in rats and mice in comparison with MSCs derived from 3D spheroids which were uniformly smaller in size (average diameter 12.6 μm).
Results We found that 3D MSCs did not cause detectable infarct in the brain as evidenced by MRI scan and TTC stain, 2D MSCs in small size caused a microinfarct in one of five animals, which was co-localized to the area of entrapped MSCs (labeled with DiI), while 2D MSCs in large size caused much larger infarcts in all five animals, and substantial amounts of DiI-positive MSCs were found in the infarct. Meanwhile, corresponding neurological defects were observed in the animals with stroke. In consistence, injection of 2D MSCs (average diameter 26.5) caused a marked loss of cortical neurons and their axons in Thy1-GFP transgenic mice and the activation of microglia in CX3CR1-GFP transgenic mice in the area with MSC entrapment.
Conclusions Our results suggest that the size of MSCs is a significant cause of MSC caused vascular obstructions and stroke.

Keywords Mesenchymal stem cells · Vascular obstruction · Cell size

Jianfeng Ge and Ling Guo contributed equally to this work

Electronic supplementary material The online version of this article (doi:10.1007/s12015-013-9492-x) contains supplementary material, which is available to authorized users.

J. Ge · S. Wang · T. Cai
School of Life Sciences, Tsinghua University, Beijing, China

J. Ge · L. Guo · S. Wang · T. Cai · Y. Wu
The Shenzhen Key Laboratory of Health Sciences and Technology, Graduate School at Shenzhen, Tsinghua University, Beijing, China

Y. Zhang
Department of Orthopedics, The General Hospital of Chinese People's Liberation Army, Beijing, China

R. C. H. Zhao
Department of Cell Biology, Institute of Basic Medical Sciences, Chinese Academy of Medical Sciences and School of Basic Medicine, Beijing, China

Y. Wu (✉)
L406A, Tsinghua Campus, The University Town, Shenzhen, China
e-mail: wu.yaojiong@sz.tsinghua.edu.cn

Introduction

Stroke is a major cause of morbidity and mortality worldwide. Most patients suffer from neurological deficits even after the most advanced therapies currently available [1, 2]. Transplantation of mesenchymal stem cells (MSCs) following experimental stroke has been shown to improve functional and structural recovery [3, 4].

MSCs are self-renewing and multipotent [5, 6]. Residing in various tissues, MSCs likely participate in the maintenance of stem cell niches and tissue homeostasis [7, 8]. Increasing evidence has suggested a profound therapeutic potential of MSCs for a variety of diseases such as myocardial infarction and stroke [9–11]. Moreover, MSCs show low immunogenecity and transplantation of allogeneic MSCs appear not to cause immune rejections [12]. For these reasons, MSCs are emerging as an extremely promising therapeutic agent and numerous clinical trials for variety of diseases are underway [11].

Intravascular delivery of MSCs has been the most popular route for MSC transplantation in clinical trials [13]. However, increasing evidence has indicated that MSCs cause considerable vascular obstruction following intravascular injection. Upon intravenous infusion, over 80 % of MSCs are entrapped in the lungs, and only less than 1 % of MSCs are detected in the ischemic heart or brain [14, 15]. Intra-arterial injection which facilitates higher levels of cell engraftment to the target organ may represent a more effective route for cell transplantation [16–19]. However, intracoronary delivery of MSCs has been found to cause acute myocardial infarction in dogs and reduction of coronary blood flow in pigs [20, 21]. Similarly, intracarotid arterial infusion of MSCs caused a marked reduction in blood flow and the development of microstrokes in rats [22]. Therefore, it has become an increasing concern over the safety of intravascular administration of MSCs.

The mechanisms of vascular obstruction of MSCs have not been fully understood. Recently, we found that intra-carotid injection of MSCs cultured in 3D spheroids which were much smaller than MSCs cultured in 2D monolayer did not cause stroke. We proposed that the size of MSCs after culture expansion might be a cause of vascular obstruction. In this study, we fractionated MSCs that had been cultured in monolayer for six passages into small and large cell populations according to their sizes, and examined their influences on vascular obstruction and the development of stroke after intra-carotid injection in rats. Our results indicated that large MSCs caused much higher incidence of stroke, more severe vascular obstruction and much larger infarct of the brain, compared to small MSCs and 3D cultured MSCs. Our results suggest that the size of MSCs in 2D monolayer culture is a significant cause of vascular obstruction.

Materials and Methods

Animals

Sprague–Dawley rats (250–270 g, purchased from the Laboratory Animal Centre, Guangdong province, China) were used for most experiments. Transgenic mice Tg(Thy1-EGFP)MJrs/J and B6.129P-*Cx3cr1*^{tm1Litt}/*J* (The Jackson Laboratory) were used to observe changes of cortical neurons and microglia after intra-ICA injection of MSCs. All animals were maintained in a temperature controlled environment (20±1 °C) with access to food and water throughout the experiment. All procedures were performed with the approval of the Animal Ethics Committee of Tsinghua University.

MSC Culture and Cell Size Fractionation

Human MSCs were isolated from human placenta as described previously [23]. Briefly, term (38–40 weeks' gestation) placentas from healthy donors were harvested with written informed consent and the procedure was approved by the Ethics Committee of XiLi Hospital. The placental tissue was washed several times with cold phosphate-buffered saline (PBS) and then mechanically minced and enzymatically digested with 0.25 % trypsin-EDTA for 30 min at 37 °C in a water bath. The digest was subsequently filtered, pelleted and resuspended in a growth medium consisting of Dulbecco's modified Eagle's medium (DMEM, Gibco-Invitrogen), 10 % fetal bovine serum (FBS; Gibco-Invitrogen) and antibiotics. Cells were seeded on uncoated polystyrene dishes (2D monolayer culture) and medium was replaced every 2 days to reach 80 % confluence. Cells were subcultured after trypsinization. Cells derived from two donors were used for experiments.

To form 3D spheroids, passage 5–7 hMSCs were cultured by a hanging drop method as described previously [24] with modifications. Briefly, 3000 hMSCs in 35 μL growth medium per drop were plated in hanging drops and incubated form 36 h to form spheroids. Then the spheroids were transferred to a suspension culture with fresh growth medium and incubated for 24 h. To obtain single cells from spheroids, spheroids were incubated with 0.25 % trypsin/EDTA for 6–10 min (depending on size of spheroids) with gentle pipetting every 2–3 min. MSCs were labeled with fluorescence DiI (Sigma) [25].

Cell size fractionation was carried out on ice. To avoid aggregation, MSCs for transplantation were prepared immediately before injection. Monolayer MSCs were trypsinized and resuspended in MSC growth medium and filtered with a nylon filter with 10 μm pores (MN10047H, German). The cells failed to pass through the filter on the top side of the membrane were collected after washing with PBS and named large MSCs (2D-L). They were filtered with a nylon cell strainer with 40 μm pores (BD) immediately before injection. The cells that passed through the pores were collected and filtered again with a nylon membrane with 7 μm pores. The cells that passed through the pores were collected and termed small MSCs (2D-S). To measure cell size, single MSCs were spread on tissue culture plate and photographed under microscope (x400). The diameter of 200 MSCs was measured using software Image J and the average diameter (mean ± SD) was calculated.

Cell Transplantation

Animals were anesthetized with 1 % pentobarbital sodium (12.5 μl/g) and stabilized on a surgical table in supine position. The common carotid artery, the external carotid artery, and the internal carotid artery (ICA) were exposed. The pterygopalatine artey branching off the ICA was ligated and the occipital artery branching off the proximal segment of the external carotid artery was dissected and coagulated. For cell injection, a vascular clip was applied to the ICA proximal to the pterygopalatine artery with the ligation of the proximal

segments of the external carotid artery and the common carotid artery. A catheter was inserted into the common carotid artery. Cells were injected immediately after the removal of the clip. 3×10^5 MSCs in 100 μl PBS per mouse, or 5×10^5 MSCs in 500 μl PBS per rat, were injected into the ICA in 2.5 min. Equal volume of PBS was injected in the control group. After transplantation, the catheter was removed and the arteriotomy site was ligated to prevent bleeding.

Two-Photon Microscopy

Two-photon microscopy imaging of neurons and microglia in the cortex of the brain in transgenic mice following intra-ICA injection of MSCs were performed according to methods previously described [26]. Briefly, 48 or 72 h after intra-ICA injection of 3×10^5 DiI-labeled MSCs, the mouse was anesthetized with 1 % pentobarbital sodium (12.5 μl/g) by intraperitoneal injection. The hair over the scalp was shaved and an incision at the midline of the scalp was cut, which extended from the level of the ears to the frontal portion of the head (between the eyes). The soft tissues on the skull were carefully removed by gently scraping the skull with a blunt microsurgical blade. The skull was placed in a skull holder which was then attached to a skull immobilization device. The exposed area of the skull was immersed with a drop of artificial cerebrospinal fluid and the skull over the region of interest (typically 0.5–1 mm in diameter and 20–50 μm in thickness) was thinned with a high-speed micro-drill under a dissecting microscope. The mouse along with the entire skull immobilization device was carefully moved to the microscope stage and visualized under two-photon laser scanning microscope for DiI-labeled MSCs and green fluorescence protein (GFP)-expressing neurons or microglia in the cortex with excitation of 920 nm and 890 nm wavelength.

Magnetic Resonance Imaging

The development of strokes after intra-ICA injection of MSCs was assessed by magnetic resonance imaging (MRI, a clinical 3.0 T MR system, Magnetom TIM Trio, Siemens, Erlangen) with a custom rat coil. T2-weighted sequences (T2-TSE) were performed at each MRI session consisting of 23 transverse slices (TR: 4000 ms, TE: 82 ms, FOV: 42×60 mm; slice thickness: 1 mm). All sequences were measured with a multicontrast-spin echo (se-mc) sequence. For further processing, MRI sequences were exported as DICOM sequences.

2, 3, 5-Triphenyltetrazolium Chloride Assay

Forty eight hours after intra-ICA injection of MSCs, rats were anesthetized and decapitated. Their brains were removed and coronally sectioned into six 2-mm coronal slices, incubated for 30 min in a 1 % solution of 2, 3, 5-triphenyltetrazolium chloride (TTC, Sigma-Aldrich) at 37 °C, and fixed with 4 % PFA in PBS. Infarct areas were measured by using software Image J and infarct volumes were calculated, which was presented as infarct volume per volume of the entire cerebral hemisphere.

Whole Mount of Retina and Iris

Forty eight hours after intra-ICA injection of DiI-labeled MSCs, rats received tail vein injection of fluorescein isothiocyanate-dextran (500000 MW; 100 mg/kg; Sigma-Aldrich) to label blood vessels, and sacrificed shortly. The left retina and iris were carefully removed, mounted on glass slides, fixed with 4 % paraformaldehyde (PFA) [27], and visualized under fluorescence microscope (Leica).

Behavioral Tests

Each rat was subjected to the modified neurological severity score (mNSS) test according to a method reported previously [3, 28]. The score was determined by parameters of motor (muscle status and abnormal movement), sensory (visual, tactile placement and proprioceptive), and reflex tests (pinna, corneal and startle reflex). One point was awarded for the inability to correctly perform a task or for the lack of a tested reflex.

Stem Cell Tracking with Microscopy Video

To visualize vasculature, 50 μl FITC-Dextran (500000 MW, Sigma-Aldrich) was injected into the tail vein of Balb/C mice (18–22 g) 5 min before cells injection. To image MSCs trafficking in the blood vessels of the iris, mice were anesthetized, and the head of mouse was fixed on the platform of the microscope (Leica AF7000). The eyelids of mouse were opened up with a self-made mental circular device. The laser beam from a 10× objective lens was focused at the iris. The carotid artery was prepared and a catheter was inserted for injection of MSCs. 0.5×10^6 DiI-labeled MSCs in 100 μl 1 % BSA/PBS was injected slowly into the catheter, and the cells passing through the blood vessels in the iris were video imaged simultaneously with a 549 nm excitation laser for DiI and a 488 nm excitation laser for FITC-dextran.

Statistical Analysis

All data were expressed as mean ± standard deviation (SD). One-way ANOVA was used for data analysis and statistical significance was defined as $P<0.05$.

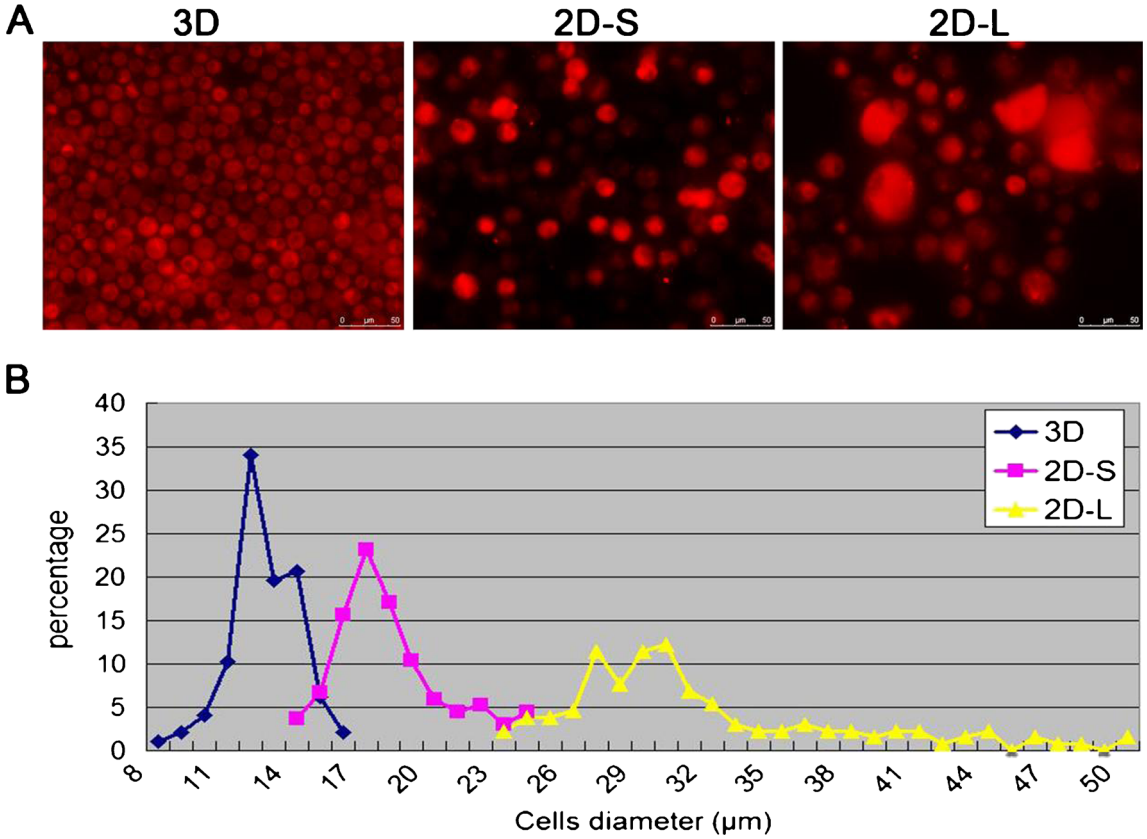

Fig. 1 Sizes of MSCs. **a** Representative images of single MSCs derived from passage 6 monolayer which were fractionated according to their sizes into small (2D-S) and large (2D-L) cells. Passage 6 MSCs became uniformly smaller after 60 h of 3D spheroid culture (3D). **b** Diameter distribution of MSCs

Results

Size Fractionation of MSCs

The sizes of passage 6 MSCs that had been cultured in monolayer widely scattered among 15–50 μm in diameter, with an average diameter of 26.5±0.4 (Fig. 1a and b). The MSCs were size fractionated by two nylon filters with different pore sizes. We found that live MSCs could pass through filters with pores much smaller than their sizes. As the percentage of MSCs with a diameter less than 15 μm was minor, we first sorted for MSCs smaller than 20 μm which passed through a filter with 7 μm pores. The sizes of these cells were 14-24 μm, and their average diameter was 17.9±0.2 (2D-S, Fig. 1a and b). These cells took 41.4 % of passage 6 MSCs and were termed small cells. 20.7 % MSCs failed to pass through a filter with 10 μm pores. Their sizes were 23–50 μm, with an average diameter of 30.4± 0.5 μm (Fig. 1a and b), and these cells were named large cells (2D-L). MSCs that had been cultured in monolayer for six passages were further cultured in 3D spheroids for 60 h and then dispersed into single cells. These 3D MSCs became uniformly smaller with an average diameter of 12.6±0.2 μm (Fig. 1a and b).

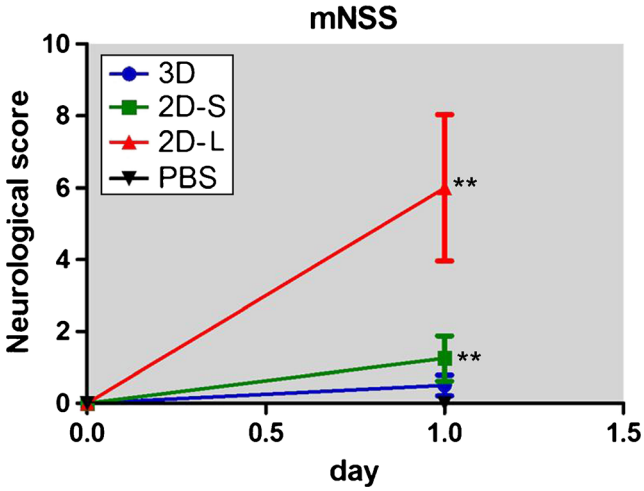

Fig. 2 mNSS scores. Evaluation of mNSS scores in rats 24 h after intracarotid injection of 5×10^5 MSCs with different sizes. 2D-S, small MSCs derived from monolayer (n=5); 2D-L, large MSCs derived from monolayer (n=5); 3D, MSCs derived from 3D spheroid culture (n=5). PBS, injection of equal volume of PBS (n=4). $^{**}P<0.01$, 2D-L and 2D-S vs PBS or 3D

The Association of MSC Size with Vascular Obstruction and Strokes

To examine whether the size of MSCs affected the severity of vascular obstruction and the incidence of MSC-caused strokes, we injected 5×10^5 3D MSCs, 2D monolayer cultured small (2D-S) or large (2D-L) MSCs into the ICA in rats (five rats in each group) and observed the outcomes. As the velocity of MSC infusion has been suggested to be a potential cause of stroke, we injected MSCs at a low speed 200 μl/min. Prior to cell injection, there was no neurological defect in all rats (mNSS=0 in each group). Twenty four hours after cell injection, rats injected with PBS remained neurologically normal (mNSS=0), rats received an injection of 3D MSCs developed minor neurological deficits in two of five animals (average mNSS=0.4±0.2), rats injected with small MSCs (2D-S) showed moderate decreases in mNSS in four of five animals (average mNSS=1.5±0.5), and all rats received an injection of large MSCs (2D-L) developed evident neurological defect (average mNSS=6.0±1.6, $P<0.05$) (Fig. 2) with the death of one animal 5 h after cell injection.

Twenty four hours after cell injection, of five rats in each group, MRI analysis showed that no strokes developed in all 3D MSC-injected animals, one rat in the 2D-S MSC-injected group developed a single lacunar stroke in the middle cerebral artery supplied region ($n=5$), and all five animals developed various degrees of strokes in the 2D-L MSC-injected groups in the middle cerebral artery supplied region (Fig. 3a). TTC stain of the brain sections at 48 h following cell injection showed consistent results with the MRI data (Fig. 3b).

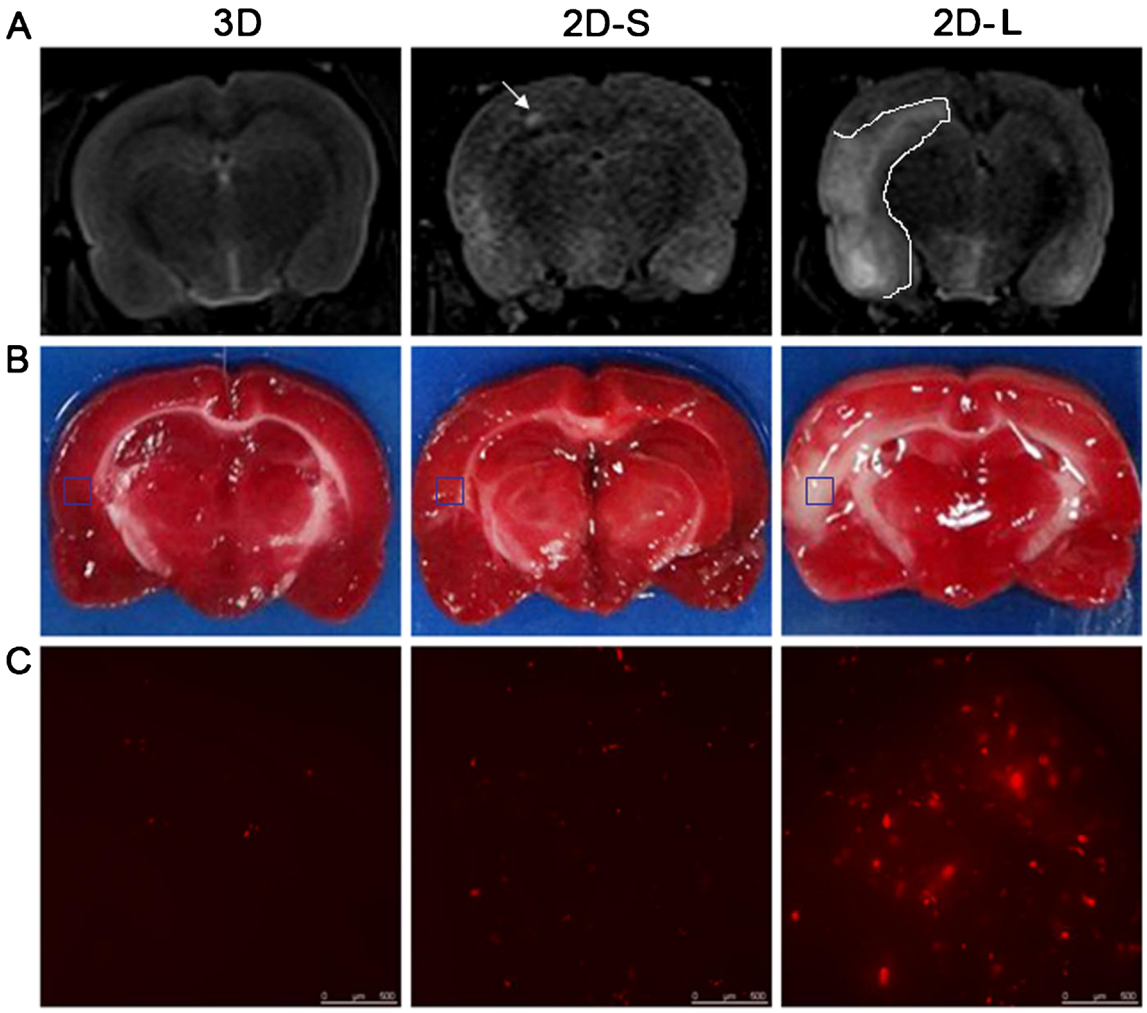

Fig. 3 Evaluation of stroke and MSC entrapment. Twenty four hours after intra-carotid injection of 5×10^5 MSCs with different sizes (2D-S, small MSCs derived from monolayer; 2D-L, large MSCs derived from monolayer; 3D, MSCs derived from 3D spheroid culture) in rats ($n=5$ each), the development of stroke was assessed by MRI and TTC stain. **a** Representative images of MRI scan. *Whitish areas* represent infarcts in the middle cerebral supplied cortical and sub-cortical areas. *Arrow* in 2D-S indicates a lacunar stroke lesion. **b** Representative images of TTC stain. Large damaged areas in the cortex and sub-cortex in 2D-L. **c** Representative fluorescence microscopic images of the region corresponding to the stroke showing the presence of DiI-positive MSCs (*red*); the abundance of DiI-MSCs in the brain appeared to positively correlated with the incidence and size of stroke

Detection of DiI-labeled MSCs in the brain sections showed that a substantial amount of DiI-positive cells in the infarct in rats injected with large 2D MSCs, while little DiI-MSCs were observed in rats received small 2D MSCs or 3D spheroid MSCs (Fig. 3c).

To observe the real time influences of intra-ICA injection of MSCs on cerebral cells in the brain cortex, we injected DiI-labeled MSCs to thy1-GFP transgenic mice whose cortical neurons specifically expressed GFP in the cytoplasm and CX3CR1-EGFP transgenic mice whose microglia specifically expressed GFP. Two-photon microscopy imaging of the brain cortex in the middle cerebral artery supplied region at 48 h following cells injection in thy1-GFP transgenic mice showed a dramatic loss of the GFP-positive neurons along with their axons extending toward the cortex surface in areas with the entrapment of DiI-positive MSCs in all mice injected with MSCs derived from 2D monolayer culture with an average diameter of 26.5 μm (2D, n=8), and such areas were easily found in these mice. In mice received injection of MSCs derived from 3D spheroids, DiI-positive MSCs were barely detected in the cortex and the organization of the cortex neurons and axons appeared similar to that in the PBS injected animals (Fig. 4a). In consistence, examination of microglia in CX3CR1-EGFP transgenic mice 72 h after cell injection showed marked morphological changes of microglia in areas with MSC entrapment in rats received MSCs derived from 2D monolayer. These microglia became significantly enlarged in their bodies and thicker in their processes, representing the activated state of microglia. Meanwhile, in animals injected with MSCs derived from 3D spheroids, the microglia appeared similar in morphology to those in the PBS-injected animals (Fig. 4b). Moreover, we also examined the trafficking of DiI-labeled MSCs in the blood vessels of the iris in wild type mice who received an injection of FITC-Dextran prior to cell injection to illuminate the vasculature. The trafficking of DiI-MSCs was recorded by a video camera under fluorescence microscope. MSCs derived from 3D spheroids moved fast and smoothly in the blood vessels, while MSCs derived from monolayers moved much slower and some stopped moving in the blood vessels (Supplementary video 1).

We further examined vascular obstructions in the iris and retina of rats 48 h after intra-ICA injection of 5×10^5 MSCs which were pre-labeled with DiI under fluorescence microscope, and found that DiI-positive cells were barely detected in the iris (Fig. 5a) and retina (Fig. 5b) of rats injected with 3D MSCs, only a few DiI-positive cells were detected in animals received the injection of small MSCs derived from 2D monolayer culture (2D-S), and abundant DiI-positive MSCs were observed in the vasculature (probably arterioles and capillaries) of the iris and retina of animals injected with large

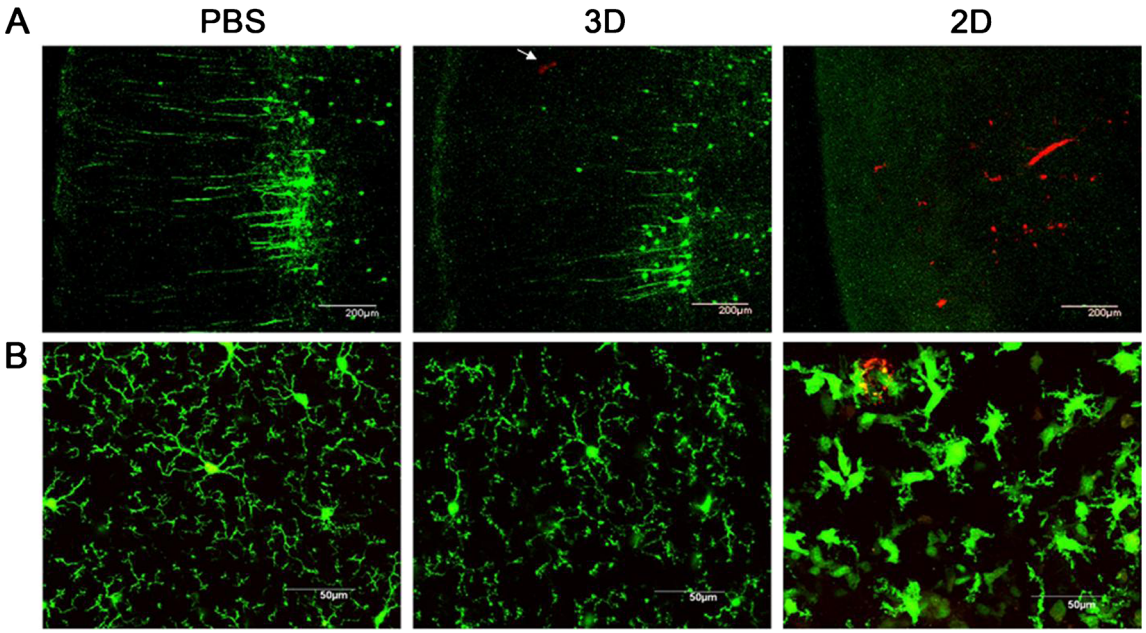

Fig. 4 Changes of cortical neurons and microglia after injection of MSCs. Two-photon microscopy imaging of the brain cortex in the middle cerebral artery supplied region was performed 2 or 3 days after the injection of 3×10^5 DiI labeled MSCs in different sizes (2D, MSCs derived from monolayer; 3D, MSCs derived from 3D spheroid culture) or PBS in live thy1-GFP (**a**) or CX3CR1-EGFP (**b**) transgenic mice. In PBS injected thy1-GFP transgenic mice, GFP-positive neurons along with their axons (*green*) extending toward the cortex surface were clearly detected. **a** In mice received injection of 2D MSCs, a dramatic loss of the GFP-positive neurons along with their axons was observed in areas with the entrapment of DiI-positive MSCs (*red*). In mice received injection of MSCs derived from 3D spheroids, DiI-positive MSCs were barely found in the cortex and the organization of the cortex neurons and axons appeared normal. **b** Microglia (*green*) became significantly enlarged in their bodies and thicker in their processes in the area with the entrapment of DiI-MSCs in mice received injection of 2D MSCs. In mice injected with MSCs derived from 3D spheroids, microglia appeared similar in morphology to those in the PBS-injected animals

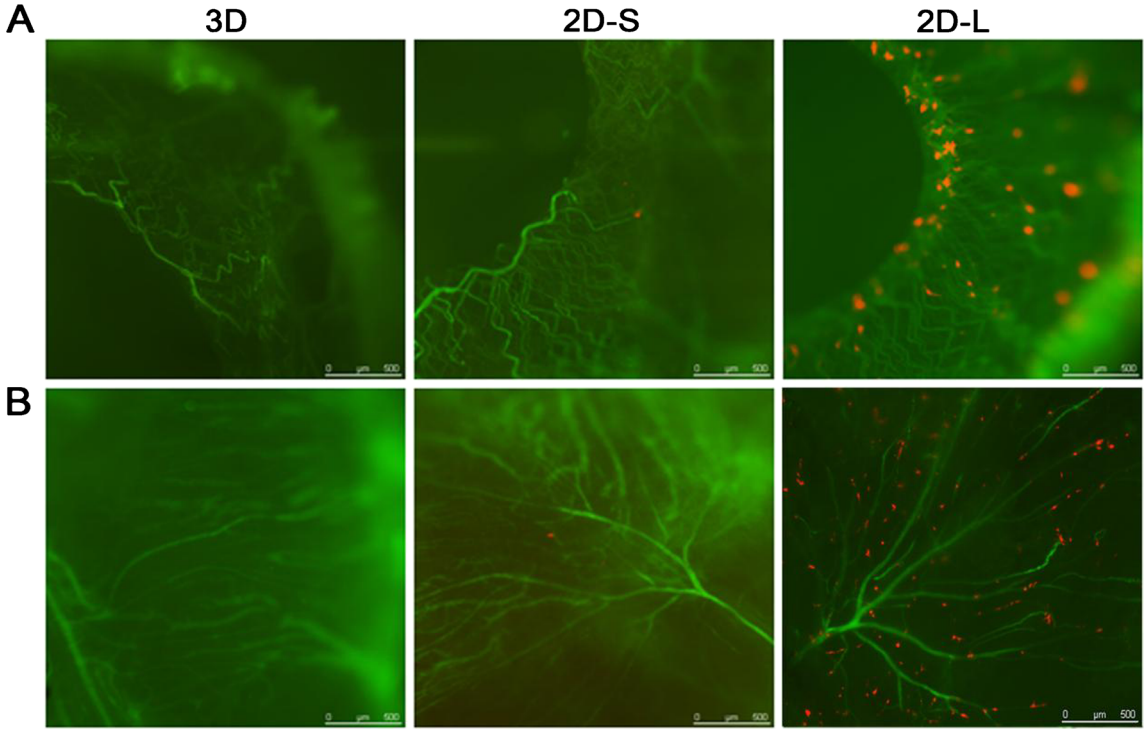

Fig. 5 Vascular obstructions of MSCs. Two days after the injection of 5×10^5 DiI-MSCs with different sizes (2D-S, small MSCs derived from monolayer; 2D-L, large MSCs derived from monolayer; 3D, MSCs derived from 3D spheroid culture) in rats, MSCs retained in the iris (**a**) and retina (**b**) were examined under fluorescence microscope. The vasculature (*green*) was labeled by fluorescein isothiocyanate-dextran. Abundant DiI-positive MSCs (*red*) were found in the iris and retina of rats injected with 2D-L cells, which were largely localized inside the vasculature. Little or no DiI-MSCs were detected in rats received 2D-S MSCs or 3D MSCs

MSCs derived from 2D monolayer culture (2D-L) (Fig. 5a and b).

Discussion

MSCs have been found to cause severe vascular obstructions after intra-vascular injection in large and small animal models. The mechanisms of vascular obstruction of MSCs have been poorly understood. The size of MSCs after successive culture in monolayer had been assumed to be a cause, but direct evidence lacked. In this study, we fractionated MSCs cultured in 2D monolayer according to their sizes, and show that intra-ICA injection of small MSCs derived from 2D monolayer (average diameter 17 μm) or MSCs derived 3D shperoids (which were uniformly smaller with an average diameter of 13 μm) caused minimal or no vascular obstructions and stroke, respectively, while intra-ICA injection of large MSCs (average diameter 29 μm) derived from 2D monolayer caused severe vascular obstructions and stroke in rats, indicating that the size of MSCs is a significant determinant of MSC-caused vascular obstructions.

Intra-arterial delivery of MSCs facilitates more efficient engraftment of the cells into target organs than intravenous injection, but appears to be associated with more serious outcomes of vascular obstruction. In a previous study, following an intra-ICA injection of MSCs derived from monolayer in rats, up to 41 % of animals died, while only 8 % of animals died after intravenous administration [29]. Similarly, in another study, intra-ICA injection of culture expanded MSCs caused a significant (80–90 %) reduction of the blood flow to the brain in 35 % of rats and led to subsequent death of these animals [22]. In the present study, we found that all rats received intra-ICA injection of large MSCs developed stroke, which were evidenced by typical ischemic changes in MRI and TTC stain in the middle cerebral artery supplied region of the brain, and defects in neurological function. In consistence, severe vascular obstructions were found in the iris and retina of the eye (supplied by an artery derived from the ICA) in these animals.

The size of MSCs significantly increases after successive culture expansion in monolayer. The average diameter of MSCs in passage 6 MSCs that had been successively cultured in monolayer was 26.5 μm, which was similar to that in published literature [24]. This size is about two to three times larger than leukocytes [30], potentially increasing the difficulty of the cells to pass through capillaries. In consistence with our observation, a recent study showed that intra-ICA injection of smaller glial-restricted precursors (diameters 13–15 μm), which were much smaller that MSCs (average diameter 25 μm), did not cause evident reduction in cerebral blood flow, while similarly injected MSCs caused a profound reductions cerebral blood flow [31].

Though glial-restricted precursors are expected to significantly differ from MSCs in many aspects, the results imply the significance of cell size in MSC caused vascular obstruction. Our results, using MSCs derived from the same culture passage but in different sizes clearly indicate that the severity of vascular obstruction and the incidence of stroke are positively correlated with the increase in MSC size. Moreover, in consistence with previous studies [24], we found that the size of MSCs that had been expanded in monolayer for several passages could be dramatically reduced after a period of culture in 3D spheroids. These cells became uniform in size and generally smaller than the population of smallest MSCs before 3D culture. Injection of these cells caused no vascular obstruction and stroke.

We clearly demonstrated the loss of neurons and the activation of microglia in the area of the cortex with MSC entrapment in live transgenic mice. Thy1-GFP transgenic mice whose cortical neurons specifically expressed GFP in the cytoplasm serve as an ideal model to examine changes of cortex neurons and their axon organizations [32]. We found a dramatic loss of neurons and their axons in areas with the presence of large MSCs. Along with these changes was the presence of activated microglia in the CX3CR1-EGFP transgenic mice in the area with large MSCs. Microglia are known to be activated in the cerebral lesion following ischemic stroke and undergo a series of morphological changes [32, 33]. With this model, we demonstrated the morphological changes of microglia in the ischemic cortex in live animals, which were similar to those reported in the ischemic lesion after stroke [32, 33].

In conclusion, with MSCs in different sizes, we showed that the incidence and severity of MSC-caused vascular obstructions and stroke after intra-carotid injection was closely relative to their sizes. As the size of MSCs that have been expanded in monolayer can be substantially reduced after an episode of culture in 3D spheroids, the use of small MSCs is practical and potentially increases the safety of intra-vascular transplantation of MSCs.

Acknowledgments This work was supported by grants from Natural Science Foundation of China (No. 30871273, 31371404, U1032003) and Shenzhen Science and Technology Innovation Committee (JC201005280597A, GJHZ20120614194251967 and JCYJ20130402145002397) to Y Wu.

Conflict of interest The authors have declared that no conflict of interest exists.

References

1. Hacke, W., Kaste, M., Bluhmki, E., Brozman, M., Davalos, A., Guidetti, D., et al. (2008). Thrombolysis with alteplase 3 to 4.5 hours after acute ischemic stroke. *The New England Journal of Medicine, 359*, 1317–1329.
2. Zhang, Z. G., & Chopp, M. (2009). Neurorestorative therapies for stroke: underlying mechanisms and translation to the clinic. *Lancet Neurology, 8*, 491–500.
3. Li, Y., Chen, J., Wang, L., Lu, M., & Chopp, M. (2001). Treatment of stroke in rat with intracarotid administration of marrow stromal cells. *Neurology, 56*, 1666–1672.
4. van Velthoven, C. T. J., Sheldon, R. A., Kavelaars, A., Derugin, N., Vexler, Z. S., Willemen, H. L. D. M., et al. (2013). Mesenchymal stem cell transplantation attenuates brain injury after neonatal stroke. *Stroke, 44*, 1426–1432.
5. Horwitz, E. M. (2006). MSC: a coming of age in regenerative medicine. *Cytotherapy, 8*, 194–195.
6. Prockop, D. J. (1997). Marrow stromal cells as stem cells for nonhematopoietic tissues. *Science, 276*, 71–74.
7. Chamberlain, G., Fox, J., Ashton, B., & Middleton, J. (2007). Concise review: mesenchymal stem cells: their phenotype, differentiation capacity, immunological features, and potential for homing. *Stem Cells, 25*, 2739–2749.
8. Keating, A. (2012). Mesenchymal stromal cells: new directions. *Cell Stem Cell, 10*, 709–716.
9. Chen, J., Li, Y., Wang, L., Zhang, Z., Lu, D., Lu, M., et al. (2001). Therapeutic benefit of intravenous administration of bone marrow stromal cells after cerebral ischemia in rats. *Stroke, 32*, 1005–1011.
10. Mangi, A. A., Noiseux, N., Kong, D., He, H., Rezvani, M., Ingwall, J. S., et al. (2003). Mesenchymal stem cells modified with Akt prevent remodeling and restore performance of infarcted hearts. *Nature Medicine, 9*, 1195–1201.
11. Salem, H. K., & Thiemermann, C. (2010). Mesenchymal stromal cells: current understanding and clinical status. *Stem Cells, 28*, 585–596.
12. Uccelli, A., Moretta, L., & Pistoia, V. (2008). Mesenchymal stem cells in health and disease. *Nature Reviews Immunology, 8*, 726–736.
13. Wu, Y., & Zhao, R. C. (2012). The role of chemokines in mesenchymal stem cell homing to myocardium. *Stem Cell Reviews, 8*, 243–250.
14. Lee, R. H., Pulin, A. A., Seo, M. J., Kota, D. J., Ylostalo, J., Larson, B. L., Semprun-Prieto, L., Delafontaine, P., & Prockop, D. J. (2009). Intravenous hMSCs improve myocardial infarction in mice because cells embolized in lung are activated to secrete the anti-inflammatory protein TSG-6. *Cell Stem Cell, 5*, 54–63.
15. Toma, C., Wagner, W. R., Bowry, S., Schwartz, A., & Villanueva, F. (2009). Fate of culture-expanded mesenchymal stem cells in the microvasculature: in vivo observations of cell kinetics. *Circulation Research, 104*, 398–402.
16. Bliss, T., Guzman, R., Daadi, M., & Steinberg, G. K. (2007). Cell transplantation therapy for stroke. *Stroke, 38*, 817–826.
17. Fischer, U. M., Harting, M. T., Jimenez, F., Monzon-Posadas, W. O., Xue, H., Savitz, S. I., et al. (2009). Pulmonary passage is a major obstacle for intravenous stem cell delivery: the pulmonary first-pass effect. *Stem Cells and Development, 18*, 683–692.
18. Guzman, R., De Los Angeles, A., Cheshier, S., Choi, R., Hoang, S., Liauw, J., et al. (2008). Intracarotid injection of fluorescence activated cell-sorted CD49d-positive neural stem cells improves targeted cell delivery and behavior after stroke in a mouse stroke model. *Stroke, 39*, 1300–1306.
19. Harting, M. T., Jimenez, F., Xue, H., Fischer, U. M., Baumgartner, J., Dash, P. K., et al. (2009). Intravenous mesenchymal stem cell therapy for traumatic brain injury. *Journal of Neurosurgery, 110*, 1189–1197.
20. Freyman, T., Polin, G., Osman, H., Crary, J., Lu, M., Cheng, L., et al. (2006). A quantitative, randomized study evaluating three methods of mesenchymal stem cell delivery following myocardial infarction. *European Heart Journal, 27*, 1114–1122.
21. Vulliet, P. R., Greeley, M., Halloran, S. M., MacDonald, K. A., & Kittleson, M. D. (2004). Intra-coronary arterial injection of mesenchymal stromal cells and microinfarction in dogs. *Lancet, 363*, 783–784.

22. Walczak, P., Zhang, J., Gilad, A. A., Kedziorek, D. A., Ruiz-Cabello, J., Young, R. G., et al. (2008). Dual-modality monitoring of targeted intraarterial delivery of mesenchymal stem cells after transient ischemia. *Stroke, 39*, 1569–1574.
23. Li, Z., Liu, C., Xie, Z., Song, P., Zhao, R. C., Guo, L., et al. (2011). Epigenetic dysregulation in mesenchymal stem cell aging and spontaneous differentiation. *PLoS One, 6*, e20526.
24. Bartosh, T. J., Ylostalo, J. H., Mohammadipoor, A., Bazhanov, N., Coble, K., Claypool, K., et al. (2010). Aggregation of human mesenchymal stromal cells (MSCs) into 3D spheroids enhances their antiinflammatory properties. *Proceedings of the National Academy of Sciences of the United States of America, 107*, 13724–13729.
25. Wu, Y., Ip, J. E., Huang, J., Zhang, L., Matsushita, K., Liew, C.-C., et al. (2006). Essential role of ICAM-1/CD18 in mediating EPC recruitment, angiogenesis, and repair to the infarcted myocardium. *Circulation Research, 99*, 315–322.
26. Yang, G., Pan, F., Parkhurst, C. N., Grutzendler, J., & Gan, W. B. (2010). Thinned-skull cranial window technique for long-term imaging of the cortex in live mice. *Nature Protocols, 5*, 201–208.
27. Powner, M. B., Vevis, K., McKenzie, J. A., Gandhi, P., Jadeja, S., & Fruttiger, M. (2012). Visualization of gene expression in whole mouse retina by in situ hybridization. *Nature Protocols, 7*, 1086–1096.
28. Tsai, L. K., Wang, Z., Munasinghe, J., Leng, Y., Leeds, P., & Chuang, D. M. (2011). Mesenchymal stem cells primed with valproate and lithium robustly migrate to infarcted regions and facilitate recovery in a stroke model. *Stroke, 42*, 2932–2939.
29. Li, L., Jiang, Q., Ding, G., Zhang, L., Zhang, Z. G., Li, Q., et al. (2009). Effects of administration route on migration and distribution of neural progenitor cells transplanted into rats with focal cerebral ischemia, an MRI study. *Journal of Cerebral Blood Flow & Metabolism, 30*, 653–662.
30. Stammers, A. D. (1926). The blood count and body temperature in normal rats. *The Journal of Physiology, 61*, 329–336.
31. Janowski, M., Lyczek, A., Engels, C., Xu, J., Lukomska, B., Bulte, J. W., et al. (2013). Cell size and velocity of injection are major determinants of the safety of intracarotid stem cell transplantation. *Journal of Cerebral Blood Flow and Metabolism, 33*, 921–927.
32. Eckert, M. A., Vu, Q., Xie, K., Yu, J., Liao, W., Cramer, S. C., et al. (2013). Evidence for high translational potential of mesenchymal stromal cell therapy to improve recovery from ischemic stroke. *Journal of Cerebral Blood Flow and Metabolism, 33*, 1322–1334.
33. Döppner, T., & Hermann. (2010). *Mesenchymal stem cells in the treatment of ischemic stroke: Progress and possibilities* (p. 157). Stem Cells and Cloning: Advances and Applications.